ESC European Society of Cardiology

European Heart Journal Open (2022) **2**, 1–7
https://doi.org/10.1093/ehjopen/oeac028

SHORT REPORT
Translational basic science

The AAV-PCSK9 murine model of atherosclerosis and metabolic dysfunction

William Coles Keeter[1], Nigeste M. Carter [2,†], Jerry L. Nadler[3], and Elena V. Galkina [1,*]

[1]Department of Microbiology and Molecular Cell Biology, Eastern Virginia Medical School, 700 West Olney Rd, LH3180, Norfolk 23507, VA, USA; [2]Department of Pharmacology and Toxicology & Toxicology, Virginia Commonwealth University, Richmond 23298, VA, USA; and [3]Department of Medicine and Pharmacology, New York Medical College, Valhalla 10595, NY, USA

Received 5 October 2021; revised 6 April 2022; online publish-ahead-of-print 20 June 2022

Handling Editor: Daniel Ketelhuth

Aims Mouse models with genetic modifications are required to investigate atherogenesis and associated metabolic syndrome. Adeno-associated virus-8 (AAV8)-mediated overexpression of PCSK9 (AAV8-PCSK9) induces hyperlipidaemia and promotes atherosclerosis in C57BL/6 mice. We aimed to assess whether AAV8-PCSK9-injected C57BL/6 mice fed high-fat diet with added cholesterol (HFD-C) would serve as a model of combined metabolic syndrome and atherosclerosis.

Methods and results C57BL/6 mice received i.v. injection of AAV-PCSK9 and sex- and age-matched *Ldlr*$^{-/-}$ and C57BL/6 control mice were placed on HFD-C or chow diet for 20 weeks (B6-PCSK9-HFD-C, *Ldlr*$^{-/-}$ HFD-C, B6-HFD-C, and B6-Chow, respectively). High-fat diet with added cholesterol feeding led to insulin resistance and impaired glucose clearance in B6-PCSK9-HFD-C mice compared with B6-Chow controls. This decrease in metabolic health in B6-PCSK9-HFD-C mice as well as the development of atherosclerosis was similar to *Ldlr*$^{-/-}$ HFD-C mice. Importantly, HFD-C feeding induced pancreatic islet hyperplasia in B6-PCSK9-HFD-C and B6-HFD-C compared with B6-Chow controls. In line with alterations in the metabolic phenotype, there was an increase in the number of pro-inflammatory Ly6C$^{high/med}$ monocytes within the adipose tissues of B6-PCSK9-HFD-C and B6-HFD-C compared with B6-Chow controls.

Conclusion High-fat diet with added cholesterol-fed AAV-PCSK9-injected C57BL/6 mice can serve as a useful model of integrated metabolic syndrome and atherosclerosis that does not require genetic manipulations.

* Corresponding author. Tel: +1 757 446 5019, Email: galkinev@evms.edu
† Present address: Department of Pharmacology and Toxicology, Virginia Commonwealth University, Richmond 23284, VA, USA.

Graphical Abstract

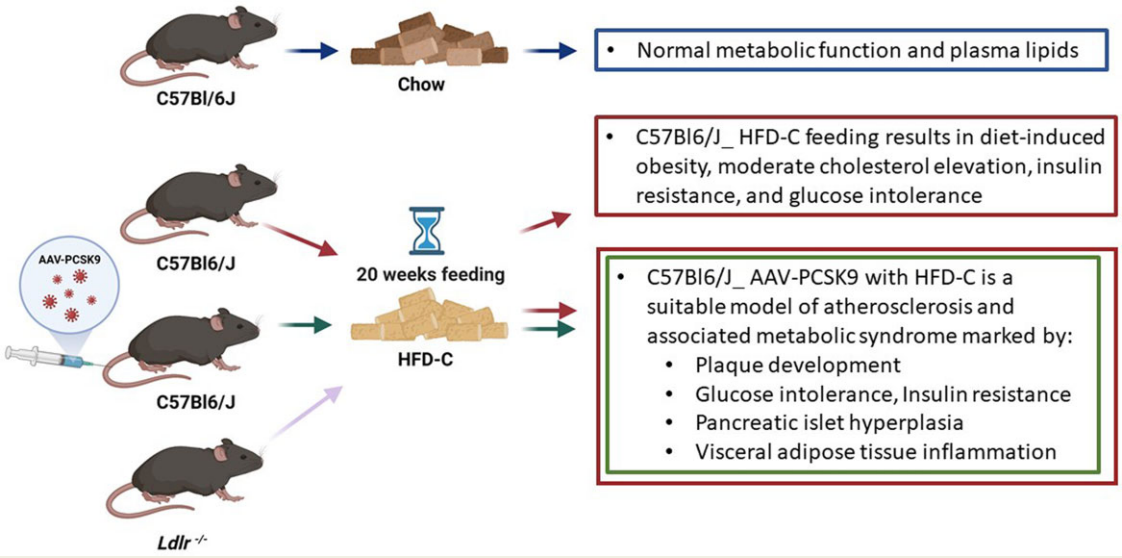

Schematic illustration of the study design with notable results. Mice with hypercholesterolemia induced by AAV-PCSK9 injection paired with high-fat diet with added cholesterol (HFD-C) display similar glucose intolerance and insulin resistance profiles compared to non-injected HFD-C fed control mice, despite having advanced atherosclerosis. Notably, AAV-PCSK9 mice fed HFD-C have mimic the metabolic deficiencies compared with popular HFD-C fed Ldlr$^{-/-}$ model of metabolic syndrome and atherosclerosis.

Keywords Hypercholesterolaemia • Obesity • Metabolic syndrome • Atherosclerosis • Inflammation

Introduction

The coincidence of cardiovascular disease and obesity-related Type-2 diabetes (T2D) is widely known.[1] Recently, a high-fat diet with added cholesterol (HFD-C) was reported as a suitable model for insulin resistance, glucose intolerance, and atherosclerosis in low-density lipoprotein receptor-deficient (*Ldlr*$^{-/-}$) mice.[2,3] While the HFD-C-fed *Ldlr*$^{-/-}$ mouse model is a great tool to study atherogenesis and insulin resistance, crossing these mice with other transgenic mice requires substantial time and resources. A novel model of atherosclerosis can bypass such crossing via a single injection of recombinant adeno-associated virus (AAV) encoding a gain-of-function mutant form of proprotein convertase subtilisin/kexin type 9 (PCSK9) that targets hepatic LDLR and causes a rapid increase of circulating cholesterol and atherogenesis when paired with high-fat diet.[4] In humans, PCSK9 levels significantly correlate with several parameters of metabolic syndrome including obesity, hypertension, fasting blood glucose, and serum insulin levels.[5] Current research aims to understand whether PCSK9 levels are a result of insulin resistance, or if PCSK9 plays a contributory role in glucose metabolism. To date, the AAV-PCSK9 model of atherosclerosis has not been evaluated as a model of metabolic syndrome and atherosclerosis. Here, we hypothesize that AAV-PCSK9-induced hyperlipidaemia and HFD-C feeding will contribute to increased glucose intolerance and insulin resistance providing a suitable model for the investigation of concomitant metabolic syndrome and atherosclerosis.

Methods

AAV-PCSK9 vector production

The PCSK9 adeno-associated virus (rAAV8/D377Y-mPCSK9) was produced at the University of North Carolina (Chapel Hill, NC, USA) using the PCSK9 gain-of-function plasmid (Addgene, #58376).[4]

Animals and study design

Eight-week-old male C57Bl/6J mice ($n = 10$), were intravenously injected via tail vein with a single dose of 1×10^{11} AAV-PCSK9 particles and placed on a high-fat diet with 0.15% added cholesterol (HFD-C; fat: 60% kcal; carbohydrate: 26% kcal, Bio-Serv, F3282). Age- and sex-matched C57BL/6 and *Ldlr*$^{-/-}$ mice (Jackson, #000664, #002207, respectively) were placed on either HFD-C or chow diet for 20 weeks. Glucose tolerance (GTT, 2 g/kg) and insulin tolerance (ITT, 5 mU/g) tests were performed at 20 weeks HFD-C feeding as described previously.[3] Mice were given 2 days recovery between ITT and GTT testing, and tissues were collected 1 week later. Aortas were excised and stained for atherosclerotic lesions using Oil Red O and the percent area occupied by lesions was determined using ImageJ.[3] All animal protocols were approved by the EVMS Institutional Animal Care and Use Committee.

Plasma lipid analysis

Concentrations of total cholesterol (TC, Wako, #999-02601), LDL (LDL-C, Crystal Chem, #79980), triglycerides (TG, Cayman Chemical, #10010303) were measured in plasma of non-fasted or

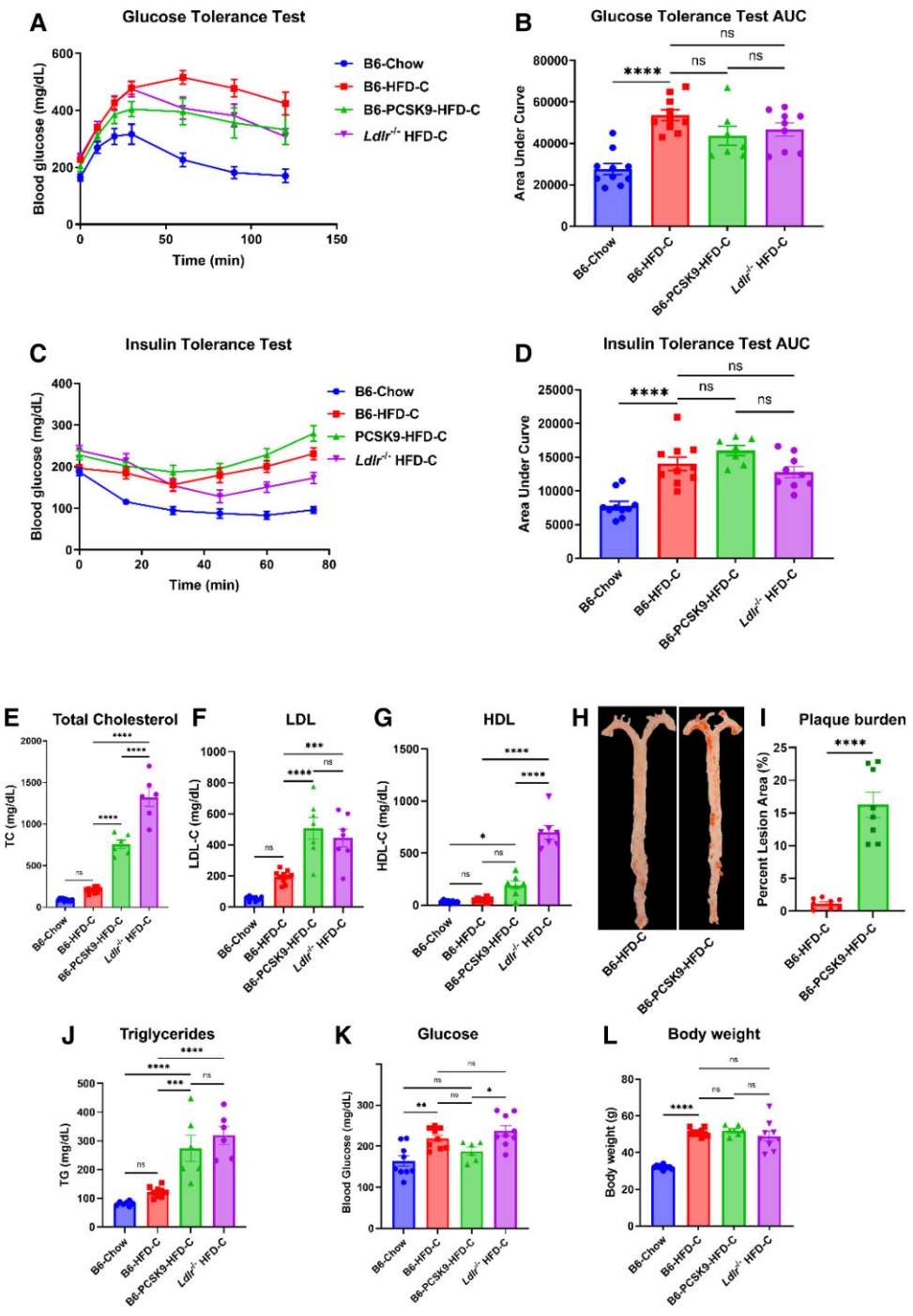

Figure 1 High-fat diet with added cholesterol-fed AAV-PCSK9-injected C57BL/6 mice represents a combined model of metabolic syndrome and atherosclerosis. (*A–D*) Time course data of blood glucose for insulin tolerance and glucose tolerance tests with area under the curve measurements. (*E–G*) Fasting total cholesterol, LDL, and HDL levels. (*H*) Representative images of *en face* aortas and (I) quantification of plaque area. (*J–K*) Fasting plasma triglyceride and glucose levels. (*L*) Body weight at 20 weeks high-fat diet with added cholesterol feeding. One-way ANOVA with Sidak's multiple comparisons test was used for statistical analysis.*$P < 0.05$, **$P < 0.01$, ***$P < 0.001$, ****$P < 0.0001$. $n = 6$–10 mice/group.

16 h-fasted mice. HDL (HDL-C) level was calculated based on the TC, LDL, and TG levels using the Friedewald equation. B6-PCSK9-HFD-C mice that achieved <300 mg/dL TC were omitted from the study ($n = 3$).

Histological analysis of islet architecture

Formalin-fixed pancreas was stained with anti-insulin antibodies (Cell Signaling Technology #4590S), then with secondary antibodies (ThermoFisher, #A21206), and islet size/number was determined using

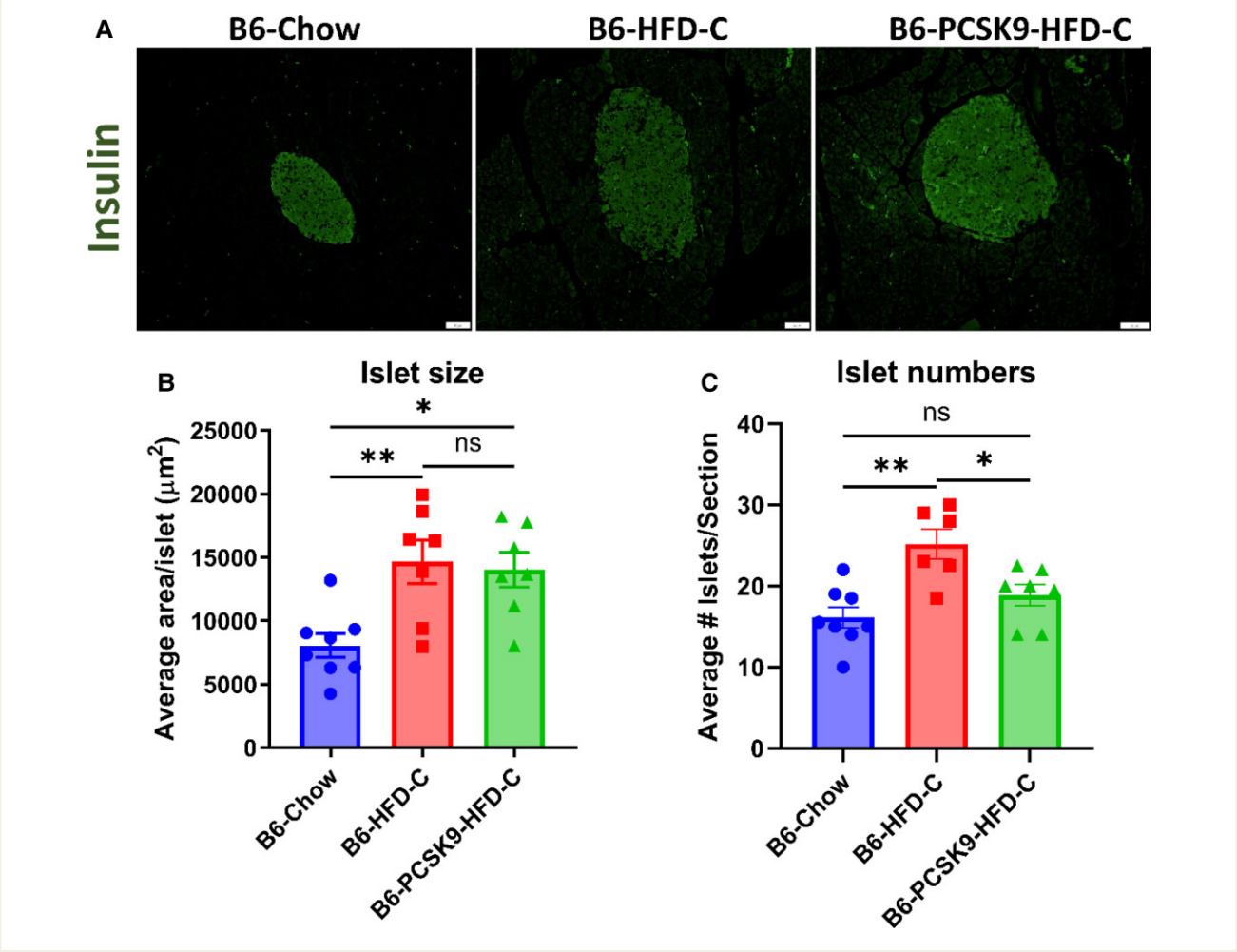

Figure 2 Increased islet size in B6-HFD-C and B6-PCSK9-HFD-C mice. (*A*) Representative islet images from whole pancreas sections stained for insulin. Scale bar = 20μm. (*B*) Average islet area and (*C*) islet numbers per section. One-way ANOVA with Sidak's multiple comparisons test was used for statistical analysis. *$P < 0.05$, **$P < 0.01$. $n = 7$–8 mice/group.

Olympus cellSens software. Two sections of the pancreas greater than 200 μm apart (average 15–25 islets/section) were used for analysis.

Flow cytometry of digested adipose tissues

Epididymal adipose tissues (AT) were digested as previously described,[6] and single-cell suspension was stained for CD45 and a Ly6C marker for pro-inflammatory Ly6C$^{high/mid}$ monocytes (Biolegend, #103130, #128006), analyzed via FACSCalibur (BD Biosciences/Cytek Inc.), and FlowJo analysis software (Tree Star Inc.). B6-Chow AT data represent two mice pooled together.

Statistics

Data are reported as mean ± SEM. One-way ANOVA with Sidak's multiple comparisons test was used for statistical comparisons between the groups. All data sets were tested and confirmed for Gaussian distribution via the Shapiro–Wilk test. Outliers were determined as mean ± 1.5×SD. Statistical significance was set at $P < 0.05$.

Results

To initially establish the effects of HFD-C feeding on metabolic parameters, C57BL/6 mice underwent ITT and GTT testing after 20 weeks of either chow (B6-Chow) or HFD-C diet feeding. B6-HFD-C mice showed a significant insulin resistance and impaired glucose tolerance compared with B6-Chow mice (*Figure 1A–D*). Next, we investigated the concomitant impact of HFD-C feeding and hypercholesterolaemia on the development of metabolic dysfunctions in HFD-C fed AAV-PCSK9 (B6-PCSK9-HFD-C) mice. Our data demonstrate that achieved levels of insulin resistance and glucose intolerance in B6-PCSK9-HFD-C mice were comparable to levels of metabolic dysfunctions in HFD-C-fed *Ldlr*$^{-/-}$ mice (*Figure 1A–D*). Interestingly, B6-PCSK9-HFD-C and *Ldlr*$^{-/-}$ HFD-C mice showed some improvement in glucose homeostasis compared with B6-HFD-C at later time points (*Figure 1A and C*); however, the area under curve was not statistically significant (*Figure 1B and D*). Thus, combinatory effects of elevated hypercholesteraemia and HFD-C feeding are enough to induce metabolic phenotype in

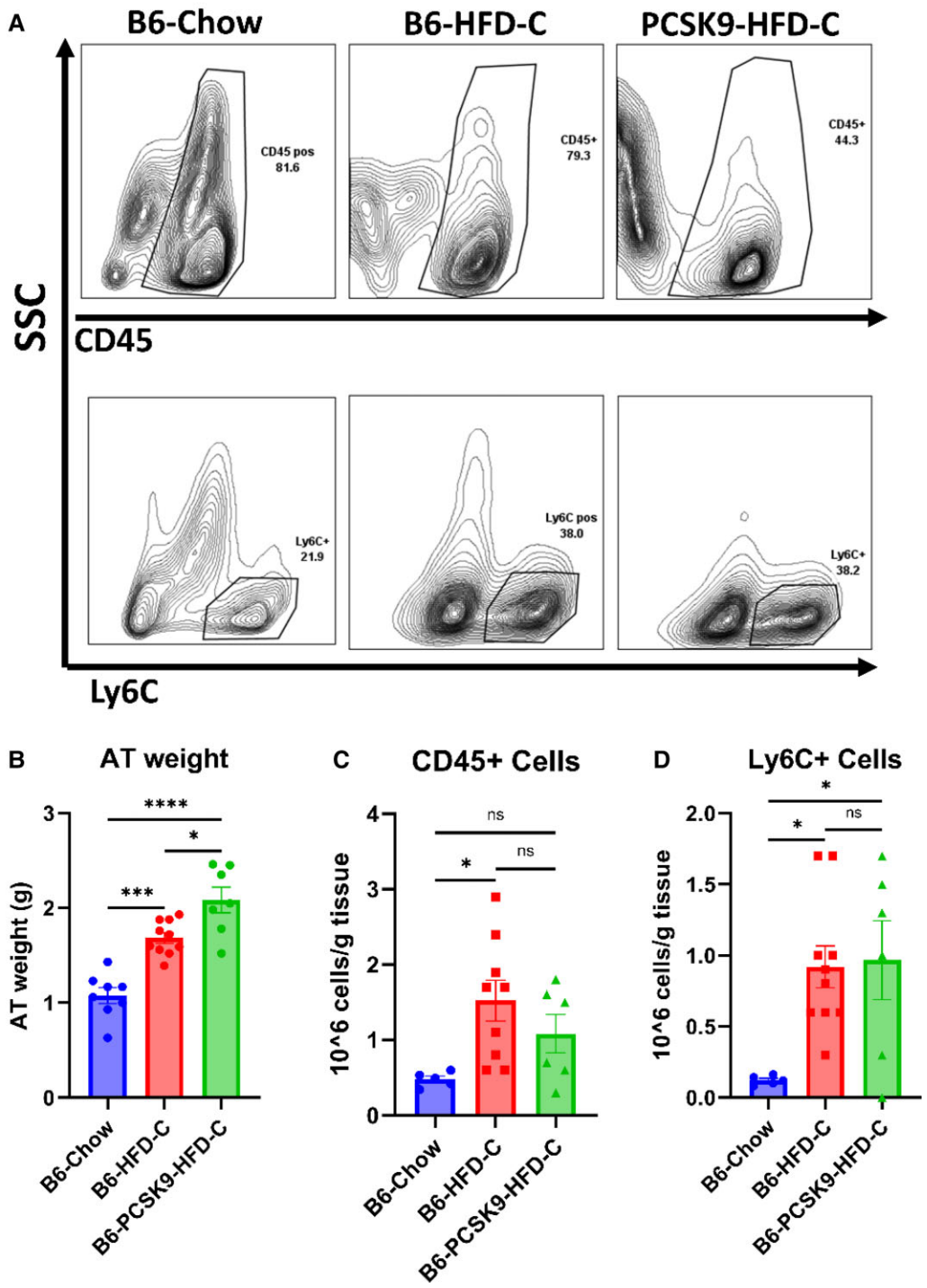

Figure 3 Increased numbers of pro-inflammatory monocytes/macrophages in AT of B6-HFD-C and PCSK9-B6-HFD-C mice. (*A*) Representative FACS plots of CD45+ leucocytes and CD45+ gated Ly6C + cells from digested adipose tissue. (*B*) Epididymal adipose tissue weight. (*C–D*) Total CD45+ and CD45+ Ly6C+ cells normalized to adipose tissues weight. One-way ANOVA with Sidak's multiple comparisons test was used for statistical analysis. *$P < 0.05$, ***$P < 0.001$, ****$P < 0.0001$. $n = 7–8$ mice/group/

C57BL/6 mice without the addition of LDLR-deficiency. High-fat diet with added cholesterol feeding induced some small lesions in B6-HFD-C mice, and the plaque development was further significantly increased in B6-PCSK9-HFD-C mice (*Figure 1H–I*). While HFD-C feeding significantly increased the body weight of B6-HFD-C mice, further elevation of TC in B6-PCSK9-HFD-C and *Ldlr*$^{-/-}$ HFD-C mice had minimal effect on body weight (*Figure 1L*). Total cholesterol, LDL, and TG levels were significantly elevated in 16 h fasted

B6-PCSK9-HFD-C and *Ldlr*$^{-/-}$ HFD-C mice vs. B6-HFD-C mice (*Figure 1E–J*), which is typically associated with decreased insulin sensitivity. HDL levels were the highest in the plasma of *Ldlr*$^{-/-}$ HFD-C mice (*Figure 1G*). Additionally, 16-h fasting glucose was increased in B6-HFD-C vs. B6-chow mice but was not further elevated in the B6-PCSK9-HFD-C and *Ldlr*$^{-/-}$ HFD-C groups (*Figure 1K*). Non-fasting TC levels were significantly increased in B6-HFD-C in comparison with B6-chow mice with further increase in B6-PCSK9-HFD-C mice (159 $\pm$ 7, 361 $\pm$ 20, and 500 $\pm$ 56 mg/dL, respectively, $P < 0.05$), whereas non-fasting TG levels were not different between these groups (112 $\pm$ 19, 125 $\pm$ 9, and 122 $\pm$ 19 mg/dL, respectively). These findings agree with previous reports whereby fasting increases TC and TG levels in mice with PCSK9 over-expression.[7] As B6-PCSK9-HFD-C mice showed a promisingly similar metabolic phenotype to *Ldlr*$^{-/-}$ HFD-C, we further investigated changes in pancreatic islet architecture as a reflection of metabolic syndrome in the PCSK9-HFD-C model.

At the initial stages of pre-diabetic conditions, insulin resistance can cause a compensatory increase in insulin production within the islets, which results in larger islet size and mass in mice.[8] In line with the metabolic profile of B6-PCSK9-HFD-C mice, an increased average islet size was observed in B6-PCSK9-HFD-C and B6-HFD-C compared with the B6-chow mice (*Figure 2A–B*). Interestingly, increased levels of TC had no further effects on islet size in B6-PCSK9-HFD-C mice compared with B6-HFD-C, yet we did observe decreased islet numbers in PCSK9-HFD-C mice (*Figure 2C*). These data suggest that high cholesterol alone has no additional effects on islet size and affects the overall number of islets.

Adipose tissues inflammation is a key contributor to peripheral insulin resistance and emigrated peripheral leucocytes are involved in inflammation within AT.[9] Therefore, we examined epididymal AT for the presence of infiltrated leucocytes and particularly monocytes/macrophages. High-fat diet with added cholesterol feeding elevated the epididymal AT mass (*Figure 3B*) and total number of CD45+ leucocytes in B6-HFD-C mice in comparison with the B6-Chow controls (*Figure 3C*), while the content of CD45+ leucocytes was not significantly elevated in B6-PCSK9-HFD-C mice likely due to normalization of number of CD45+ cells to the significantly elevated AT mass. In line with demonstrated insulin resistance and glucose intolerance in HFD-C-fed mice, we found an increased number of pro-inflammatory Ly6C$^{high/med}$ monocytes/macrophage within the AT of B6-PCSK9-HFD-C and B6-HFD-C mice compared with B6-Chow mice (*Figure 3D*).

Discussion

Rodent models of diet-induced obesity are widely used to simulate metabolic syndrome, yet limited models provide the paired conditions of atherosclerosis and metabolic syndrome.[1] Besides the HFD-C fed *Ldlr*$^{-/-}$ mice, there are only a few mouse models such as leptin- or leptin receptor-deficient mice on atherogenic background that represent a model for both T2D and atherosclerosis. Here, we show that HFD-C feeding induces a clear insulin resistance and glucose intolerance in atherosclerotic AAV-PCSK9-injected C57BL/6 mice. We further demonstrate that B6-PCSK9-HFD-C mice successfully mimicked the metabolic phenotype of HFD-C fed *Ldlr*$^{-/-}$ mice despite having lower plasma cholesterol in comparison to HFD-C fed *Ldlr*$^{-/-}$ mice. Interestingly, elevated TC in PCSK9-B6-HFD-C mice had little effect on metabolic functions compared with HFD-C-B6 mice. Collectively, our results suggest an existence of saturation levels for plasma cholesterol or the need for other lipid pathways that drive metabolic dysfunction in the conditions of HFD-C diet. Alternatively, liver-targeted modulation of PCSK9 has a limited negative impact on pancreatic islets as the local PCSK9 expression but not circulating PCSK9 regulates levels of LDLR and cholesterol content within the islets.[10] In summary, combination of HFD-C diet with AAV-PCSK9 can be used to model concomitant insulin resistance and glucose intolerance under atherosclerotic conditions.

Lead author biography

Coles Keeter received his B.S. in Integrated Science and Technology from James Madison University in 2014. He received his M.S. degree in Biotechnology from Eastern Virginia Medical School in 2015. Following 1 year of research in the biotech industry, he returned to EVMS to pursue his PhD, where his focus is on the role of neutrophils in the progression of atherosclerosis in association with metabolic syndrome. Coles plans to utilize his PhD in the pharmaceutical industry as a Medical Science Liaison.

Data availability

The corresponding author upon reasonable request will share the data underlying this article.

Acknowledgments

This work was supported by NIH R01HL142129 (E.V.G. and J.L.N.) and R01HL139000 (E.V.G.). We would like to thank Dr Imai for critically reading the manuscript. Figure illustrations were created with Biorender.

Conflict of interest: None declared.

References

1. Bornfeldt KE, Tabas I. Insulin resistance, hyperglycemia, and atherosclerosis. *Cell Metab* 2011;**14**:575–585.
2. Subramanian S, Han CY, Chiba T, McMillen TS, Wang SA, Haw A III, Kirk EA, O'Brien KD, Chait A. Dietary cholesterol worsens adipose tissue macrophage accumulation and atherosclerosis in obese LDL receptor-deficient mice. *Arterioscler Thromb Vasc Biol* 2008;**28**:685–691.
3. Taghavie-Moghadam PL, Waseem TC, Hattler J, Glenn LM, Dobrian AD, Kaplan MH, Yang Y, Nurieva R, Nadler JL, Galkina EV. STAT4 regulates the CD8(+) regulatory T Cell/T follicular helper cell axis and promotes atherogenesis in insulin-resistant Ldlr(−/−) mice. *J Immunol* 2017;**199**:3453–3465.
4. Bjorklund MM, Hollensen AK, Hagensen MK, Dagnaes-Hansen F, Christoffersen C, Mikkelsen JG, Bentzon JF. Induction of atherosclerosis in mice and hamsters without germline genetic engineering. *Circ Res* 2014;**114**:1684–1689.
5. Ferri N, Ruscica M. Proprotein convertase subtilisin/kexin type 9 (PCSK9) and metabolic syndrome: insights on insulin resistance, inflammation, and atherogenic dyslipidemia. *Endocrine* 2016;**54**:588–601.
6. Haynes BA, Huyck RW, James AJ, Carter ME, Gaafar OU, Day M, Pinto A, Dobrian AD. Isolation, expansion, and adipogenic induction of CD34 + CD31+ endothelial cells from human omental and subcutaneous adipose tissue. *J Vis Exp* 2018;**137**:57804.

7. Lambert G, Jarnoux AL, Pineau T, Pape O, Chetiveaux M, Laboisse C, Krempf M, Costet P. Fasting induces hyperlipidemia in mice overexpressing proprotein convertase subtilisin kexin type 9: lack of modulation of very-low-density lipoprotein hepatic output by the low-density lipoprotein receptor. *Endocrinology* 2006;**147**:4985–4995.
8. Roat R, Rao V, Doliba NM, Matschinsky FM, Tobias JW, Garcia E, Ahima RS, Imai Y. Alterations of pancreatic islet structure, metabolism and gene expression in diet-induced obese C57BL/6J mice. *PLoS One* 2014;**9**:e86815.
9. Guzik TJ, Skiba DS, Touyz RM, Harrison DG. The role of infiltrating immune cells in dysfunctional adipose tissue. *Cardiovasc Res* 2017;**113**:1009–1023.
10. Da Dalt L, Ruscica M, Bonacina F, Balzarotti G, Dhyani A, Di Cairano E, Baragetti A, Arnaboldi L, De Metrio S, Pellegatta F, Grigore L, Botta M, Macchi C, Uboldi P, Perego C, Catapano AL, Norata GD. PCSK9 deficiency reduces insulin secretion and promotes glucose intolerance: the role of the low-density lipoprotein receptor. *Eur Heart J* 2019;**40**:357–368.